RESEARCH ARTICLE

Choreography of the *Mycobacterium* Replication Machinery during the Cell Cycle

Damian Trojanowski,[a] Katarzyna Ginda,[a,b] Monika Pióro,[c] Joanna Hołówka,[c] Partycja Skut,[a] Dagmara Jakimowicz,[a,c] Jolanta Zakrzewska-Czerwińska[a,c]

Department of Molecular Microbiology, Faculty of Biotechnology, University of Wrocław, Wrocław, Poland[a]; Department of Biochemistry, Microbiology Unit, University of Oxford, Oxford, United Kingdom[b]; Department of Microbiology, Ludwik Hirszfeld Institute of Immunology and Experimental Therapy, Polish Academy of Sciences, Wrocław, Poland[c]

K.G. and M.P. contributed equally to this work.

ABSTRACT **It has recently been demonstrated that bacterial chromosomes are highly organized, with specific positioning of the replication initiation region. Moreover, the positioning of the replication machinery (replisome) has been shown to be variable and dependent on species-specific cell cycle features. Here, we analyzed replisome positions in *Mycobacterium smegmatis*, a slow-growing bacterium that exhibits characteristic asymmetric polar cell extension. Time-lapse fluorescence microscopy analyses revealed that the replisome is slightly off-center in mycobacterial cells, a feature that is likely correlated with the asymmetric growth of *Mycobacterium* cell poles. Estimates of the timing of chromosome replication in relation to the cell cycle, as well as cell division and chromosome segregation events, revealed that chromosomal origin-of-replication (*oriC*) regions segregate soon after the start of replication. Moreover, our data demonstrate that organization of the chromosome by ParB determines the replisome choreography.**

IMPORTANCE **Despite significant progress in elucidating the basic processes of bacterial chromosome replication and segregation, understanding of chromosome dynamics during the mycobacterial cell cycle remains incomplete. Here, we provide *in vivo* experimental evidence that replisomes in *Mycobacterium smegmatis* are highly dynamic, frequently splitting into two distinct replication forks. However, unlike in *Escherichia coli*, the forks do not segregate toward opposite cell poles but remain in relatively close proximity. In addition, we show that replication cycles do not overlap. Finally, our data suggest that ParB participates in the positioning of newly born replisomes in *M. smegmatis* cells. The present results broaden our understanding of chromosome segregation in slow-growing bacteria. In view of the complexity of the mycobacterial cell cycle, especially for pathogenic representatives of the genus, understanding the mechanisms and factors that affect chromosome dynamics will facilitate the identification of novel antimicrobial factors.**

Received 10 October 2014 **Accepted** 23 December 2014 **Published** 17 February 2015

Citation Trojanowski D, Ginda K, Pióro M, Hołówka J, Skut P, Jakimowicz D, Zakrzewska-Czerwińska J. 2015. Choreography of the *Mycobacterium* replication machinery during the cell cycle. mBio 6(1):e02125-14. doi:10.1128/mBio.02125-14.

Invited Editor William Margolin, University of Texas Medical School at Houston **Editor** Steven J. Norris, University of Texas Medical School at Houston

Address correspondence to Jolanta Zakrzewska-Czerwińska, jolanta.zakrzewska@uni.wroc.pl.

Recent years have seen significant progress in our understanding of basic bacterial cell cycle processes, particularly chromosome replication and segregation (1, 2). The application of modern fluorescence microscopy methods has allowed direct observation of replication dynamics in single bacterial cells in real time. The multiprotein replication machinery (replisome) assembled in a region of the DNA termed the replication fork is usually visualized by using fluorescent proteins fused to various DNA polymerase III holoenzyme subunits, including α (PolC), τ (DnaX) (3), χ (HolB), δ' (HolC), and β (DnaN) (3–7). To date, studies of replication dynamics have tended to focus on bacterial models such as *Bacillus subtilis*, *Escherichia coli*, and *Caulobacter crescentus*. The subcellular localization of replisomes varies among bacterial species (see Fig. 7B). In *B. subtilis* and *E. coli*, the two sister replisomes are centrally positioned shortly after the initiation of replication but localization diverges between the two species as DNA replication proceeds. In *E. coli*, replisomes move to the opposite cell halves and return to midcell at the end of replication (8, 9), whereas in *B. subtilis* (during vegetative growth), replisomes remain in the central part of the cell until the end of replication (5, 10, 11). In contrast, in *C. crescentus*, replisomes are assembled near one of the cell poles and subsequently migrate together to the cell center (4).

Unlike the case in eukaryotes, where replication and segregation events are separated in time, these cell cycle events usually take place simultaneously in eubacteria (2). In bacteria, after initiation of chromosome replication, the two copies of a newly replicated chromosomal origin (*oriC*) undergo an active asymmetric or symmetric segregation process in which one (e.g., *C. crescentus* and *Vibrio cholerae* chromosome I) or both (e.g., *E. coli*, *B. subtilis*) duplicated *oriC* regions move toward the cell pole(s) (4, 5, 8, 12). Thus, a process of concurrent replication and segregation implies that, during the bacterial cell cycle, chromosomes must undergo dynamic architectural changes. This is particularly important in

rapidly growing cells, where chromosome replication is reinitiated before the previous round of replication has been completed. As a consequence, after division, each progeny cell inherits a partially replicated chromosome with more than one chromosome origin (13). Thus far, the best-characterized components of the active segregation machinery are proteins—ParA (an ATPase) and ParB (a DNA-binding protein)—responsible for the rapid movement of sibling *oriC*'s toward a cell pole(s) soon after the start of replication (14, 15). ParB forms higher-order nucleoprotein complexes at chromosomal partitioning sites (*parS*) near *oriC* called segrosomes, which are further actively partitioned by ParA.

Chromosome replication and segregation in mycobacteria have received considerable recent research interest (16, 17). This genus of Gram-positive, GC-rich, elongated, rod-shaped bacilli encompasses slow-growing pathogens (e.g., *Mycobacterium tuberculosis*; division time, 24 h) and "fast"-growing saprophytes (e.g., *Mycobacterium smegmatis*; division time, 2 to 3 h).

In contrast to other rod-shaped bacteria, such as *E. coli* and *B. subtilis*, mycobacteria exhibit bipolar growth; their peptidoglycan is not laterally assembled but is instead exclusively incorporated at the poles (18). Additionally, mycobacteria do not possess the actin-like cytoskeletal protein MreB, which has been shown to be important for the maintenance of a rod-like cell shape in *B. subtilis* (19). Moreover, recent studies have demonstrated that mycobacterial cells can divide asymmetrically (20, 21). The phenomenon of asymmetric division raises important questions about the mechanism(s) that prevents the nucleoid from being guillotined by the asymmetrically positioned division septum. Studies on mycobacterial cell cycle processes have concentrated on the proteins involved in replication (DnaA, DnaN), segregation (ParAB), and cell division and elongation (FtsZ; Wag31, a homolog of DivIVA; PBP1a) (16, 17, 22–24). The proteins have been analyzed *in vitro* (e.g., DnaA, ParB) or *in vivo* by determining the subcellular localization of individual proteins (e.g., ParA, ParB, DnaN, FtsZ). A very recent study demonstrated that multifork replication does not occur in mycobacteria; here, individual cells are restricted to one round of chromosome replication per cell division cycle (16).

The substantial differences in growth mode and cell division between mycobacteria and better-characterized model bacteria (e.g., *E. coli*, *B. subtilis*), as well as the relative paucity of knowledge about chromosome dynamics during the mycobacterial cell cycle, prompted us to study the dynamics of chromosome replication and its coordination with other cell processes in *Mycobacterium*. Here, we investigated the subcellular localization of the chromosome replication machinery (replisomes) in real time in single cells of *M. smegmatis*, a model organism often used for studies of mycobacterial cell biology. In addition, we analyzed the influence of the ParB protein on the dynamics of chromosome replication.

(Portions of our results were presented as posters at the EMBO conference Tuberculosis 2012, Paris, 11 to 15 September 2012 [Subcellular Localization of Replisomes in *Mycobacterium*], the Gordon Research Conference Chromosome Dynamics, Lucca, 26 to 31 May 2013 [Real-Time Analysis of Replisome Dynamics in *Mycobacterium*], and the EMBO conference Microbiology after the Genomics Revolution—Genomes 2014, Paris, 24 to 27 June 2014 [Tracking Replisomes in *Mycobacterium*].)

RESULTS

***M. smegmatis* replisomes are off-centered and split during the course of replication.** To investigate whether replication is restricted to a specific intracellular region(s) and determine how this process is coordinated with the cell cycle of *M. smegmatis*, we constructed strains JH01 and DT05 expressing DnaN (sliding clamp), a subunit of DNA polymerase III, fused with green (enhanced green fluorescent protein [EGFP]) and red (mCherry) fluorescent proteins, respectively. The gene encoding DnaN was replaced with *dnaN-egfp* or *dnaN-mcherry* at the original chromosomal locus (see Text S1 in the supplemental material for details). Strains JH01 and DT05 exhibited a colony morphology and growth rate similar to those of the wild-type strain, suggesting that the fusion protein was functioning normally (see Fig. S1A in the supplemental material). The expected sizes of the fusion proteins DnaN-EGFP (75.1 kDa) and DnaN-mCherry (70.1 kDa) were observed in the cell extracts of strains JH01 and DT05, respectively (see Fig. S1A). From this, we infer that the fluorescent foci observed *in vivo* (see below) reflect the localization of the replication machinery (replisomes). Moreover, microscopic analyses revealed that the two fluorescent reporter strains showed similar patterns of replisome localization (DnaN-EGFP and DnaN-mCherry foci; see Fig. S2A and B). Thus, these strains were used to analyze the positioning of replisomes in relation to the cell cycle, chromosome segregation, and cell division.

A snapshot analysis of live DT05 (*dnaN-mcherry*) cells revealed that most of the cells in the exponential phase of growth contained either a single focus (42.3%) or double foci (35.5%) (Fig. 1A). In contrast, only a small fraction (24%) of the cells in the stationary growth phase contained fluorescent foci (see Fig. S3A in the supplemental material). The lack of fluorescent foci in the majority (76%) of the stationary-phase cells suggests that, unlike exponentially growing cells, these cells were not replicatively active. Interestingly, a small fraction of the cells—10.2 and 3.2% of those in the exponential and stationary growth phases, respectively—contained more than two foci (usually three). In most (~85%) of the cells, the distance between the two foci (replisomes) did not exceed 20% (range, 10 to 20%) of the cell length (see Fig. S3E). Cells with two foci were longer (average, 4.1 ± 0.9 μm) than those with a single focus (average, 2.7 ± 0.8 μm), particularly those in the exponential growth phase (Fig. 1; see Fig. S3B). Interestingly, DnaN foci, especially double foci, tended to be asymmetrically positioned in relation to the midcell position; a single focus was located at a position corresponding to 30 to 50% of the cell length, whereas double foci were located at positions corresponding to 25 to 50% and 40 to 65% of the cell length (Fig. 1C and D).

Considered in the light of recent reports describing mycobacterial asymmetric cell division (20, 21) and preferential elongation from the old pole (16, 20), our observations raise an interesting question about how the replication machinery is positioned in the cell in relation to the new or old pole. To investigate the relationship between the positioning of replisomes and that of cell poles, we used pulse-chase staining of the cell wall with a fluorescent amine-reactive dye (20) that stains the new pole and allows the new and old poles to be distinguished (see Fig. 2 for details). Pulse-chase staining of the *M. smegmatis* DT05 (*dnaN-mcherry*) cell wall revealed that replisomes (both single and double foci) were preferentially localized either near the midpoint of the cell (37%) or closer to the old pole (44%), with only 19% of the foci closer to the new pole (Fig. 2). It should be noted that the position of the replisomes in newborn cells is presumably determined by the old-pole-proximal localization of the *oriC* region in the predivision cell and that this is determined early on by the localization of ParB, which

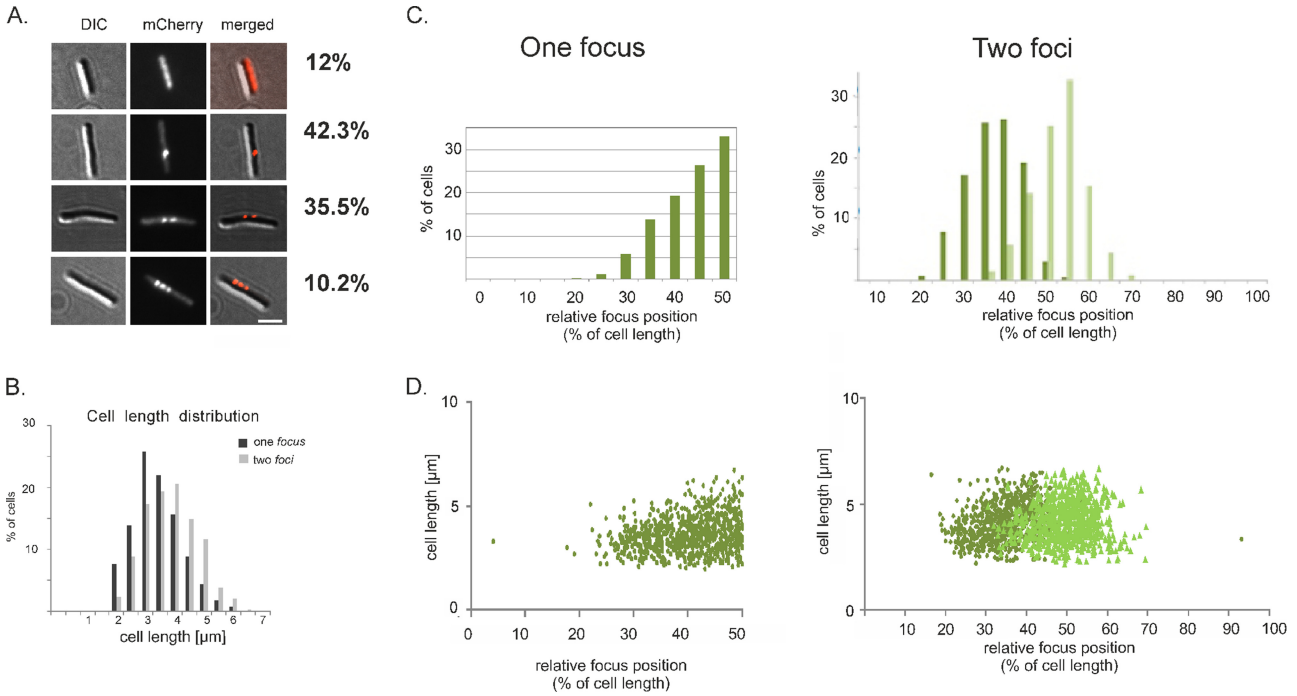

FIG 1 Localization of replisomes in relation to cell length in *M. smegmatis*. Subcellular localization of replisomes was analyzed in cells (n = 1,700) in the logarithmic growth phase. (A) Examples of cells of the *dnaN-mcherry* (DT05) strain; cells with no, one, two, or more than two DnaN-mCherry foci are shown. Left, differential interference contrast (DIC) image (Nomarski contrast); middle, red fluorescence image; right, merged DIC and fluorescence images. Scale bar, 2 μm. (B) Distribution of the lengths of cells with one focus and two foci. (C) Positions of one focus and two foci in relation to the nearest pole. (D) Quantification of focus cluster localization patterns as percentages of cell length and as a function of cell length.

binds the *parS* sequences ~5 kbp away from the *oriC* region (17). This explains why replisomes are localized proximal to the old poles in a relatively large fraction of the cells.

Replisome locations are highly dynamic. To analyze the duration and timing of chromosome replication and to explore the asymmetric nature of replication machinery positioning, we monitored the localization of DnaN-EGFP in cells (strains JH01 and PS03) growing in a microfluidic plate (ONIX flow control system) by time-lapse fluorescence microscopy (TLFM). The subcellular positions of DnaN-EGFP foci were recorded at different time intervals (Fig. 3; see also Fig. 5). Microscopic observations revealed that 8 min (on average) after its appearance, a single focus would split into two highly dynamic foci separated by a short distance (10 to 20% of the cell length) (see Fig. 5C). Prior to cell division, the foci disappeared, presumably indicating disassembly of the replication machinery (Fig. 3A and C; see also Fig. 5A). The duration of chromosome replication (C period), determined as the time from the appearance of the replisome (regarded as initiation) to the disappearance of the replisome (estimated to be termination), was calculated to be 130 to 150 min (see Fig. S1C in the supplemental material). The time between termination of replication and reinitiation in daughter cells was approximately 40 to 50 min (n = 34 cells). These data indicate an interdivision time of 170 to 200 min and suggest that replication accounts for 70% of the cell cycle.

Unlike the replisomes of *E. coli*, those of *M. smegmatis* did not segregate toward the opposite cell poles during replication; instead, they remained associated and appeared to oscillate around each other, frequently merging and splitting (Fig. 3A and C; see Fig. 5A; also see Movies S1 to S3 in the supplemental material). In the majority of the cells (71%; n = 107 cells), replication began asymmetrically relative to the cell center, closer to the old pole than to the new pole, as indicated above (Fig. 4). As replication proceeded, the two fluorescent foci, albeit highly dynamic, remained mainly in the old-pole-proximal cell half. Frequently, more than two DnaN-EGFP foci were observed, but the intensities of these "additional" foci, designated 3rd and 4th in Fig. 3, were relatively low. At a point approximately 50 to 60% through the overall replication time (i.e., 70 to 80 min; n = 35 cells), replisomes started moving toward the midcell (Fig. 4). This is consistent with the asymmetric positioning of replisomes shown by snapshot analyses and pulse-chase staining (Fig. 1 and 2), presumably owing to the fact that replisomes remained longer in the old-pole-proximal cell half than in the middle or in the new-pole-proximal half (Fig. 4).

To correlate the dynamics of replisome positioning with the cell division cycle, we constructed a merodiploid strain, DT21, expressing a PBP1a-mCherry fusion protein under the control of a tetracycline-inducible promoter (Fig. 3C and D; for details, see Text S1 and Movie S2 in the supplemental material). PBP1a (penicillin-binding protein 1a) is involved in the final stages of peptidoglycan synthesis and was recently found to be a suitable marker for real-time, live-cell imaging of apical growth and septum formation in mycobacteria (21). The growth of the DT21 strain was slightly slower than that of the parental JH01 strain, presumably because of the presence of tetracycline in the medium and/or the higher levels of PBP1a (see Fig. S1B), However, TLFM analyses revealed that the timing of replication and the reinitiation intervals in the DT21 strain were similar to those in strain JH01 (see Fig. S1C). Our microscopic analyses showed that PBP1a-mCherry localized at the cell pole(s) and septum, results similar to

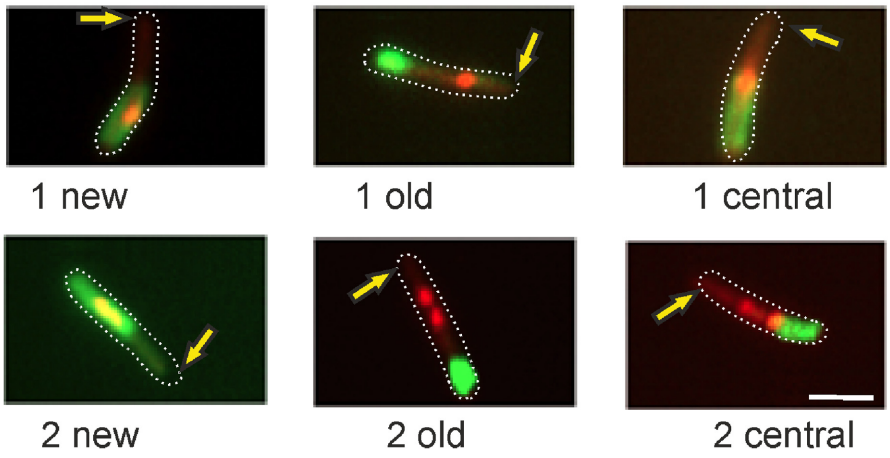

	one focus			two foci		
	new	old	central	new	old	central
% cells (1031 total)	8.0	23.7	20.0	11.3	20.3	16.9
mean cell size [μm]	3.76	3.84	3.91	4.05	4.35	4.45
SD [μm]	0.89	0.62	0.52	0.76	0.72	0.94

FIG 2 Replisome localization in relation to the new pole in *M. smegmatis*. Cell walls were pulse-labeled with a green fluorescent amine-reactive dye (20). After pulse-chase labeling, the new pole was labeled and the elongating old pole became unlabeled. Examples of DnaN-mCherry focus localization in the *dnaN-mcherry* (DT05) strain; cells with one or two foci localized in the vicinity of the central part of the cell or closer to one of the two poles (new or old) are shown. The yellow arrows indicate old poles. Scale bar, 2 μm. SD, standard deviation.

those obtained previously by Joyce et al. (21). It should be noted that septa do not form precisely in the midcell, generating cells of different sizes (21; data not shown). Moreover, time-lapse microfluidic microscopy (TLMM) analysis showed that at about 50 min after sibling cell separation (150 min after the previous cell division), PBP1a-mCherry was observed as diffuse, moving patches; after temporal condensation (~50 min), they were visible as a spot or spots in the midcell at the division site (Fig. 3D). The time interval between two consecutive PBP1a-mCherry septal-localization events—the interdivision time—was determined to be ~200 min (180 to 210 min; $n = 35$ cells), which is in agreement with the above calculations. Thus, on the basis of PBP1a-mCherry signals, we were able to more precisely measure the duration of cell cycle phases, namely, the B period phase, from cell division to the beginning of replication, and the D period phase, between the termination of replication to cell division. Approximately 10 to 20 min after the appearance of a stable PBP1a-mCherry signal at midcell ($n = 58$ cells), a single bright replisome focus appeared, suggesting initiation of chromosome replication. Approximately 30 to 40 min after replisome disassembly, the PBP1a-mCherry signal appeared at the septum of the dividing cell ($n = 31$ cells; Fig. 3C and D).

Taken together, the TLFM analysis results confirmed both the snapshot and pulse-chase staining results. Replisomes are asymmetrically positioned, being preferentially localized to the old-pole-proximal cell half. Chromosome replication is initiated approximately 15 min after septum formation (PBP1a is involved in the late stage of peptidoglycan synthesis), and replication of the entire chromosome lasts about 140 min. Finally, replication is terminated about 30 to 40 min before the appearance of a PBP1a-mCherry signal in dividing sibling cells.

ParB complexes are segregated soon after the start of replication. Our previous results demonstrated that *in vivo* ParB binds three *oriC*-proximal *parS* sequences, organizing the origin region into a compact nucleoprotein complex (segrosome) (25). ParB is detectable as either one or two complexes, depending on the segregation progress stage (17). The single ParB complex is located close to or slightly shifted from the cell center, whereas the two complexes are at positions corresponding to 20 to 25% and 75 to 80% of the total cell length. Interestingly, a TLFM analysis of *M. smegmatis* KG16 expressing ParB-mCherry revealed that segrosomes are present throughout the cell cycle, suggesting that ParB complexes are inherited ($n = 100$ cells), with each sibling cell receiving one ParB complex (K. Ginda and I. Santi, unpublished data). Since ParB binds *parS* sites located in the vicinity of the origin region, we used ParB-mCherry foci as markers for the location of *oriC*. To simultaneously analyze the positions of *oriC* and replisomes, we constructed strain PS03, expressing ParB-mCherry and DnaN-EGFP (for details, see the supplemental material). The growth of strain PS03 was similar to that of parent strain KG16 (ParB-mCherry) (17; data not shown), and the positions of DnaN-EGFP and ParB-mCherry foci were similar to those in strains JH01 and KG16, respectively (17) (Fig. 5A and B; see Movies S3 and S4 in the supplemental material). As expected, the newly assembled replisomes colocalized with the ParB focus ($n = 100$ cells; Fig. 5B), showing that replication is initiated at the *oriC*

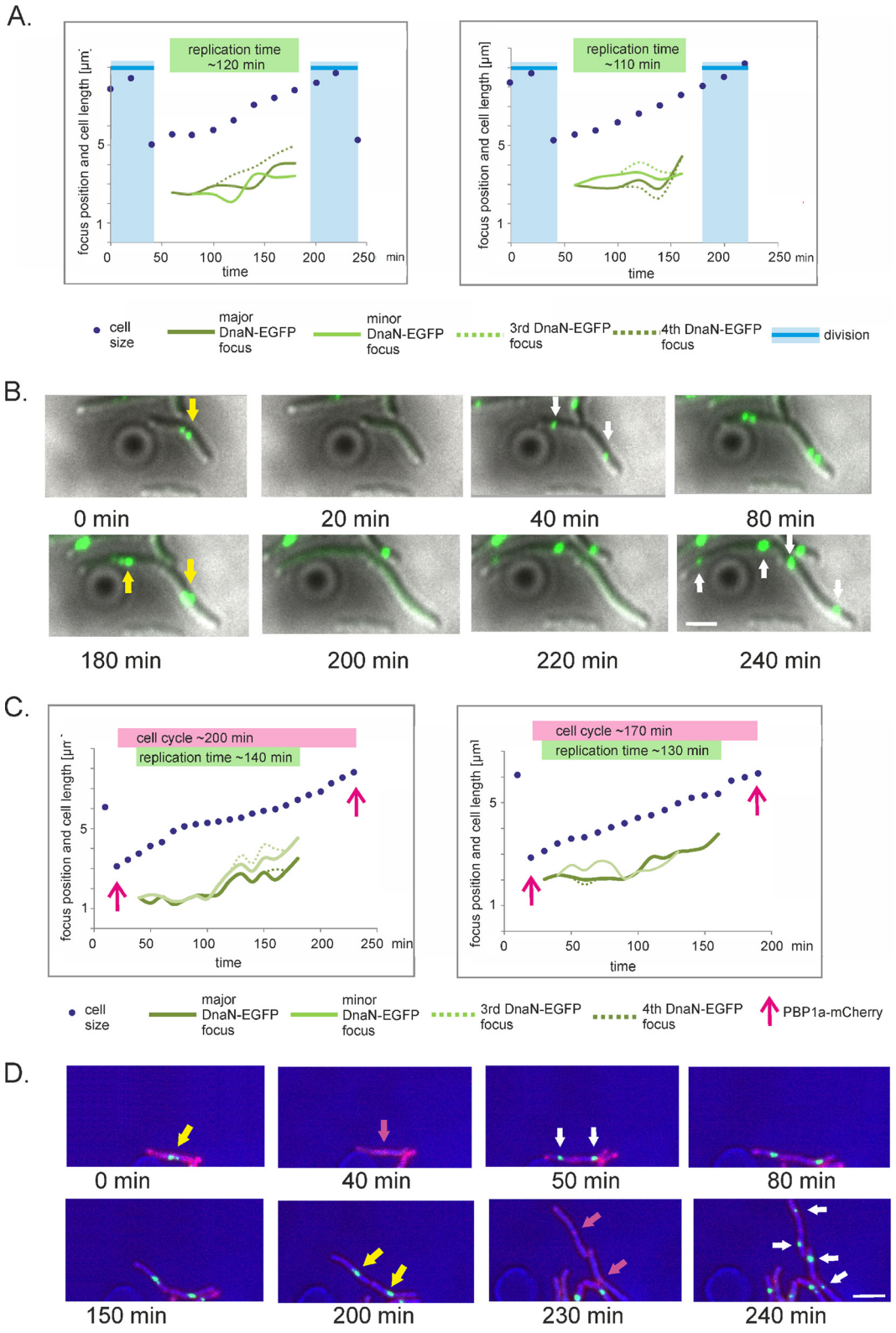

FIG 3 Replisome dynamics during the cell cycle in *M. smegmatis*. Time-lapse analysis of replisome localization during the cell cycle in strains producing either DnaN-EGFP (JH01) (A and B) or both DnaN-EGFP and PBP1a-mCherry (DT21) (C and D). Diagrams show the positions of DnaN-EGFP (solid and dotted green lines indicate major replisomes and additional replisomes emerging during replication, respectively) and cell length (dark blue dotted line) over time (20-min intervals). For ease of analysis, more-intense replisome foci are labeled "major" and less-intense foci are labeled "minor." The horizontal blue bars in panel A and the vertical pink arrows in panel C indicate consecutive cell division and PBP1a-mCherry appearance at the septum, respectively. The white, yellow, and pink arrows in panel D indicate initiation of chromosome replication, termination of chromosome replication, and septum formation, respectively. Scale bar, 2 μm.

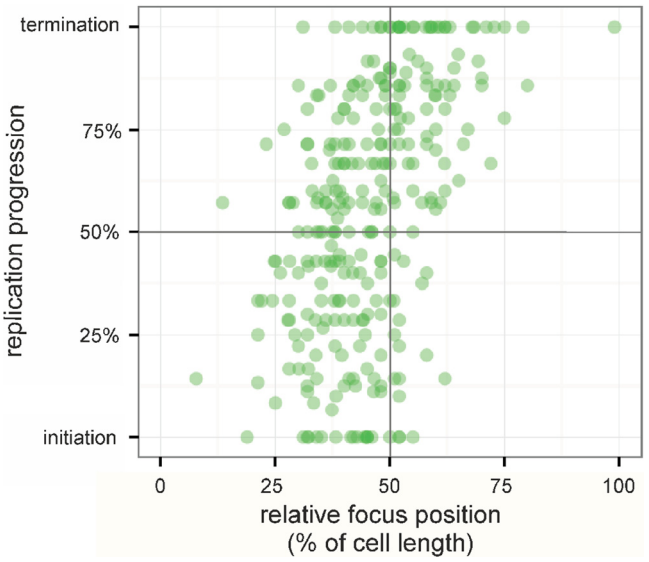

FIG 4 Relative replisome position during the replication cycle in *M. smegmatis* cells. The diagram shows the positions of DnaN-EGFP foci (in strain JH01) as a percentage of cell length. The old pole represents 0% of cell length ($n = 20$ cells).

region. Approximately 4 min after the appearance of a DnaN-EGFP focus, the ParB-mCherry focus split into two foci ($n = 115$ cells; Fig. 5D; see also Movie S4), indicating segregation of newly synthesized *oriC* regions. Four minutes later, splitting of DnaN-EGFP foci was observed. As DNA synthesis continued, daughter *oriC* regions (visible as ParB foci) migrated in opposite directions toward the cell poles, while the replisomes, positioned mainly in the old-pole-proximal cell half, oscillated locally. The movement of replisomes was similar to that observed in strain JH01 (see above). Prior to termination of replication, the replisomes were situated around the midcell. In contrast to the *oriC* regions, the replisomes split over a short distance (on average, less than 20% of the cell length) during the replication cycle.

These results confirm that replisomes are assembled near the ParB complexes, which demonstrate rapid segregation soon after the initiation of replication.

Changes in ParB levels modify the choreography of replisomes. Our observation that ParB marks the position of the *oriC* region encouraged us to test whether ParB affects the localization of the replication machinery. For this purpose, we constructed two strains that allowed us to analyze chromosome replication in cells either lacking or overproducing ParB protein. To examine replisome positioning in the absence of ParB protein, we integrated an additional copy of *dnaN* fused with the *egfp* gene into the attachment site (*attB* of mycobacteriophage L5) in the chromosome of a previously constructed strain lacking the *parB* gene (*M. smegmatis* mc^{2}155 Δ*parB*; see the supplemental material). The resulting strain was designated DT14 (see Table S1 in the supplemental material). The wild-type strain containing the integrated *dnaN-egfp* fusion gene in the same chromosome locus (DT03) was used as a control. It should be noted that the position of the DnaN-EGFP focus in the DT03 strain was similar to that observed in strains expressing the fusion protein DnaN-EGFP (JH01) or DnaN-mCherry (DT05) from its native locus (see Fig. S2). To obtain a strain overproducing ParB protein, we integrated an additional copy of the *parB* gene fused with the *mcherry* gene in the pMV306 vector into the chromosome of strain JH01 to yield the KGMD12 strain; the *parB-mcherry* fusion gene was expressed under the control of the acetamide-inducible P_{ami} promoter (see Table S1). A control strain, KGMD13, with an integrated pMV306 vector containing only the *mcherry* gene (also under the control of the inducible P_{ami} promoter) was also constructed (see Table S1).

A snapshot analysis showed that *parB* deletion (DT14) influenced replisome positioning, as did ParB overexpression (KGMD12), although to a smaller extent (Fig. 6). Interestingly, in both cases, the distances between two replisomes were larger than in the corresponding control strains (DT03 and KGMD13, respectively), although this tendency was less marked in the KGMD12 strain. Moreover, in the strain overexpressing ParB, we observed a larger fraction of the cells that were either not replicatively active (21% versus 12% in the control strain) on the basis of the absence of replisome fluorescent foci or contained three or more DnaN-EGFP foci (23% versus 15% in the control strain) (Fig. 6F). Additionally, a microscopic analysis showed that the fraction of the cells in the ParB-overexpressing strain containing one replisome focus (24%) was lower than that in the control strain (40%) (Fig. 6F).

To further investigate the influence of ParB on the localization of newly assembled replisomes, we analyzed *parB* gene deletion-containing and ParB-overexpressing strains by TLFM. In the strain lacking ParB protein, the newborn replisomes were localized more randomly than in the JH01control strain (Fig. 6C), suggesting that positioning of the *oriC* region by ParB may determine the site of replication initiation and, consequently, replisome assembly. In the case of ParB overproduction, the replication pattern was considerably changed, with a large fraction of the cells exhibiting either no or more than two DnaN-EGFP foci (similarly to the results of our snapshot analysis). The larger fraction of the cells with more than two replisomes was accompanied by an increased number of segrosomes per cell (see Movie S5 in the supplemental material). In ParB-overexpressing cells, we observed disruption of the localization pattern of inherited ParB-mCherry foci, the asynchronous appearance of DnaN-EGFP foci, and the presence of multiple ParB and DnaN foci in a large fraction of the cells (see Movie S5). These data suggest that ParB overexpression triggers changes in cell cycle events. In addition, ParB overexpression was associated with the production of small, nonviable cells without any noted increase in the fraction of anucleate cells.

In summary, our results revealed that modification of the ParB level altered the distance between split replisomes and the number of observed replisomes. These findings suggest that ParB not only contributes to the positioning of the *oriC* region but also helps control the overall chromosome organization and/or the coordination of cell cycle processes.

DISCUSSION

Evidence accumulated over the past decade suggests that, unlike replisomes in eukaryotes, those in bacteria are not stationary but dynamic (26). However, until now, studies of the dynamics of the chromosome replication machinery have focused largely on a few fast-growing bacteria (with the exception of *C. crescentus*, which is slow growing) that elongate longitudinally. In this study, we analyzed the dynamics of chromosome replication and its coordina-

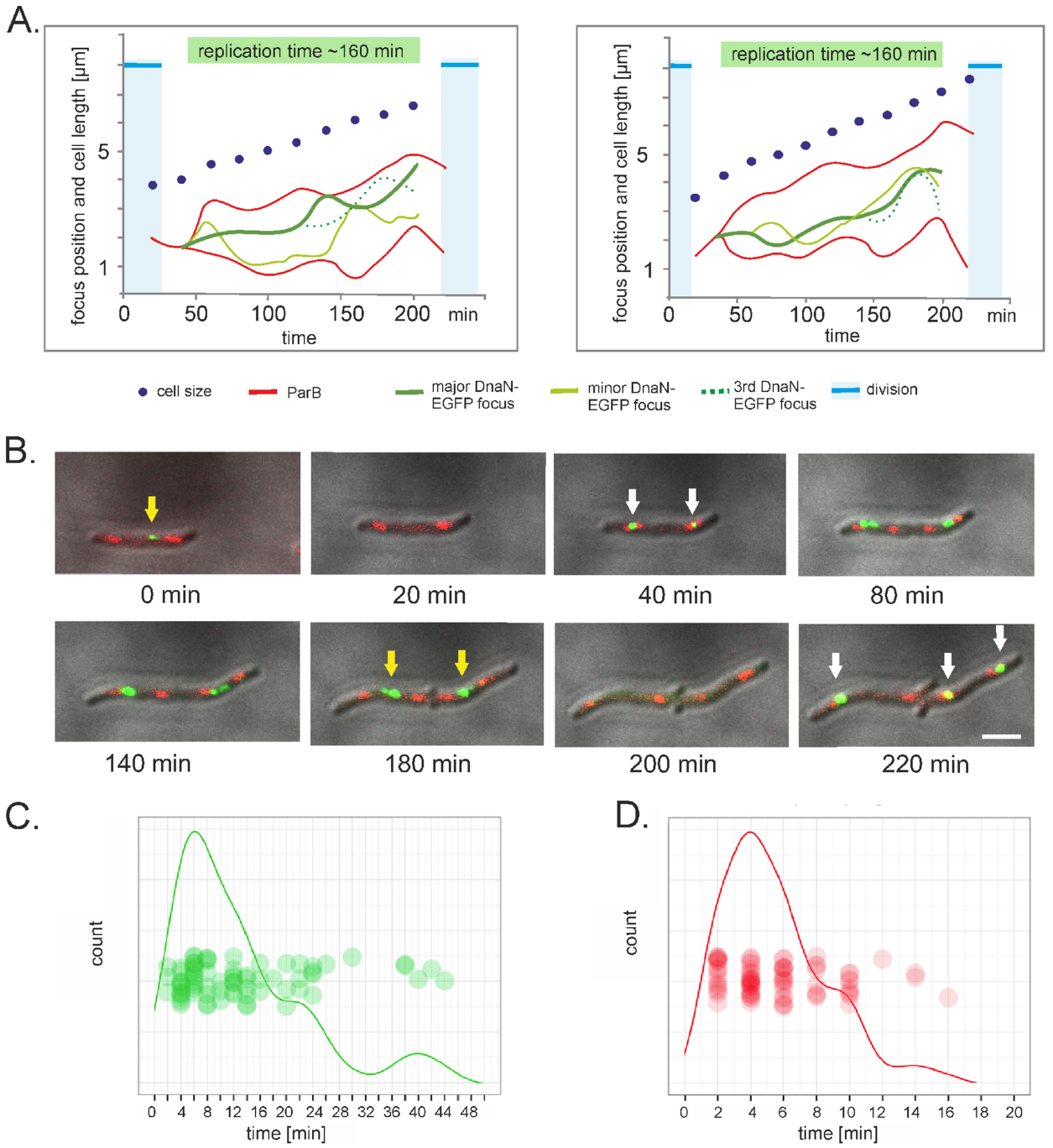

FIG 5 Replisome dynamics in relation to ParB position during the cell cycle in *M. smegmatis*. (A and B) Time-lapse analysis of replisome (green) and ParB (red) localization during the cell cycle of PS03 strain producing DnaN-EGFP and ParB-mCherry. (A) Diagrams show the positions of replisomes (solid and dotted green lines indicate major replisomes and additional replisomes emerging during replication, respectively), ParB (red line), and cell length (dark blue dotted line) over time (10-min intervals). The horizontal blue bars indicate cell division. (B) The white and yellow arrows indicate initiation and termination of chromosome replication, respectively. Scale bar, 2 μm. (C and D) Diagrams show times of DnaN-EGFP and ParB-mCherry focus separation, respectively, after the appearance of replisomes in newborn cells (imaging interval, 2 min; DnaN-EGFP and ParB-mCherry foci were analyzed in 126 and 115 cells, respectively).

tion with segregation and cell division in single cells of *M. smegmatis*—a slow-growing, pole-elongating bacterium.

Our data indicate that *M. smegmatis* cells undergo only one round of replication per cell cycle; the next round of DNA synthesis is not initiated until the previous round of replication has finished (n >100 cells). Chromosome replication lasts about 140 min, which is ~70% of the cell cycle duration, and in the majority of cells, replication is initiated approximately 15 min after cell division (B period), which is defined as septum formation (Fig. 7A). Replication is terminated about 40 min (D period) before cell wall synthesis at the septum of dividing cells. Interestingly, Santi et al. previously reported that replication is initiated in

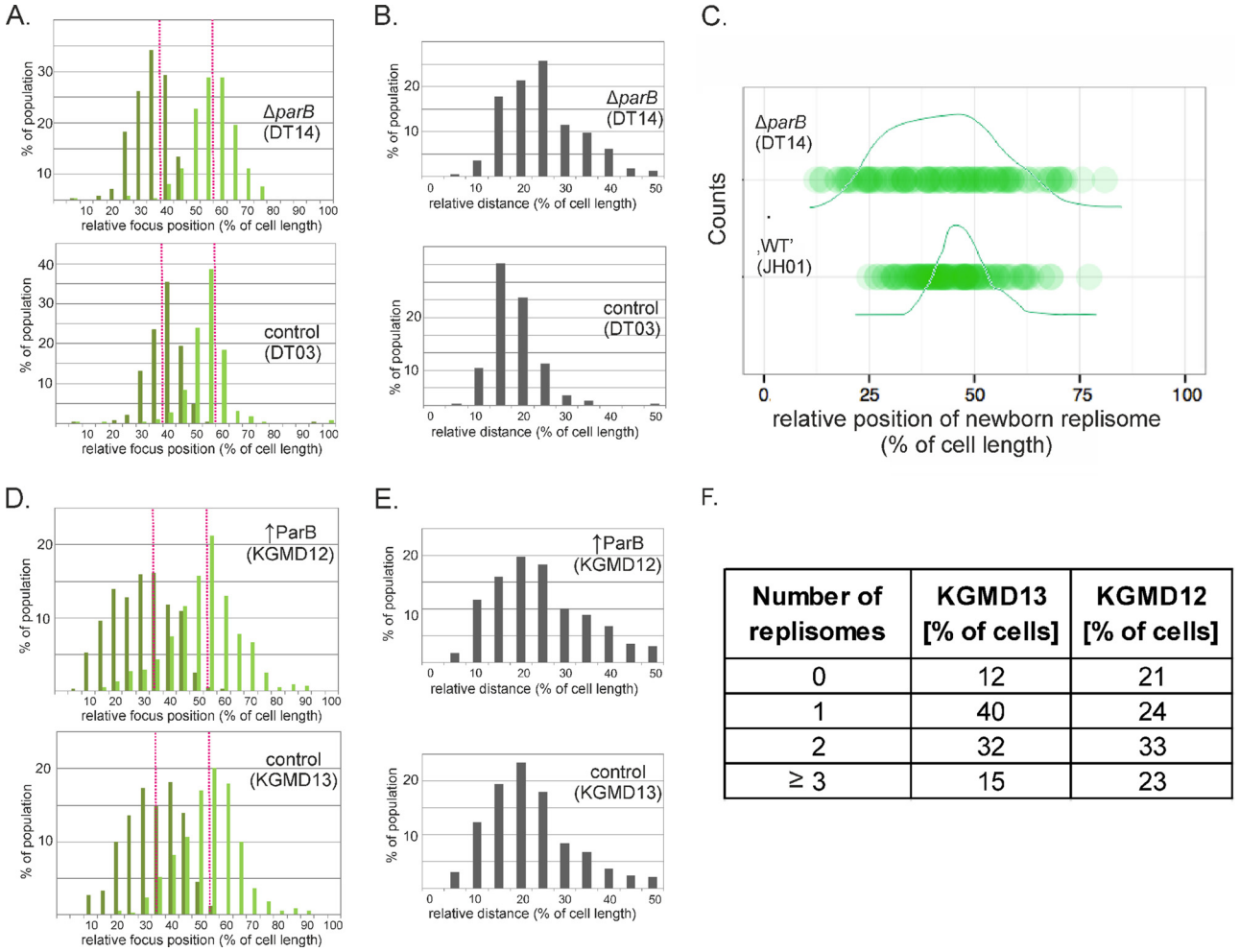

Number of replisomes	KGMD13 [% of cells]	KGMD12 [% of cells]
0	12	21
1	40	24
2	32	33
≥ 3	15	23

FIG 6 Influence of ParB elimination or overexpression on replisome positioning in *M. smegmatis* cells. (A and D) Positions of two DnaN-EGFP foci in relation to the nearest pole in the Δ*parB* strain (DT14) and in the strain overproducing ParB-mCherry (KGMD12). (B and E) Distances between two DnaN-EGFP foci in the Δ*parB* strain (DT14) and in the strain overproducing ParB-mCherry (KGMD12). (C) Diagram showing the positions of newly formed replisomes in the Δ*parB* strain (DT14) and the wild-type (WT) strain (JH01). (F) Frequencies of cells with no, one, two, or more than two replisomes in the strain overexpressing ParB protein (KGMD12) compared with the control strain (KGDM13).

the mother cell prior to cell division (but after termination of the previous replication round) and is completed in sibling cells (16). We also observed this phenomenon, but only in a small fraction (15%) of the *M. smegmatis* cells analyzed ($n = 65$ cells; data not shown). This discrepancy may reflect the use of PBP1a as a cell division marker in our studies instead of DivIVA (Wag31), which was employed by Santi et al. It is likely that DivIVA localizes to the septum at a later stage of cell division, potentially explaining the apparent differences between these reports. In agreement with results obtained previously (16), the length of the C period indicates that the DNA synthesis rate is about 400 bases (b)/s, which is similar to the rate determined for *Myxococcus xanthus* (370 b/s) (27) and *C. crescentus* (350 b/s) (28), organisms that also undergo only one round of replication per cell cycle. In contrast, the DNA synthesis rate in *B. subtilis* and *E. coli*, fast-growing bacteria capable of multifork replication (13), was estimated to be 600 to 1,000 b/s, and under optimal growth conditions, up to 12 replication forks could be present on the same chromosome. Interestingly, the rate of DNA synthesis of *M. tuberculosis* (~50 b/s) (29, 30) is about 8 times slower than that of *M. smegmatis*. The activity of *M. tuberculosis* DNA polymerase III is not likely to be the rate-limiting factor, since all of the subunits of the holoenzyme show high homology with the corresponding subunits from *M. smegmatis*. Thus, one possible explanation for the slower DNA synthesis of *M. tuberculosis* might be limited availability to nucleotides.

In newborn cells, the initial position of the replisome is presumably determined by the position of the *oriC* region at the time of initiation. We used ParB-mCherry foci as a marker of the origin region, since ParB forms nucleoprotein complexes in close proximity to *oriC* that are inherited by the daughter cells. Indeed, we found that newly assembled replisomes, visible as single foci, colocalize with the ParB complex; they are slightly asymmetrically located in relation to the midcell, being closer to the old pole than to the new pole. Approximately 4 min after the initiation of replication, the newly synthesized *oriC* regions (visualized as ParB-mCherry foci) segregate in opposite directions, and after the next 4 min, the replisomes split (Fig. 5 C and D). Interestingly, in *E. coli*, the newly replicated DNA, particularly the *oriC* region, is held

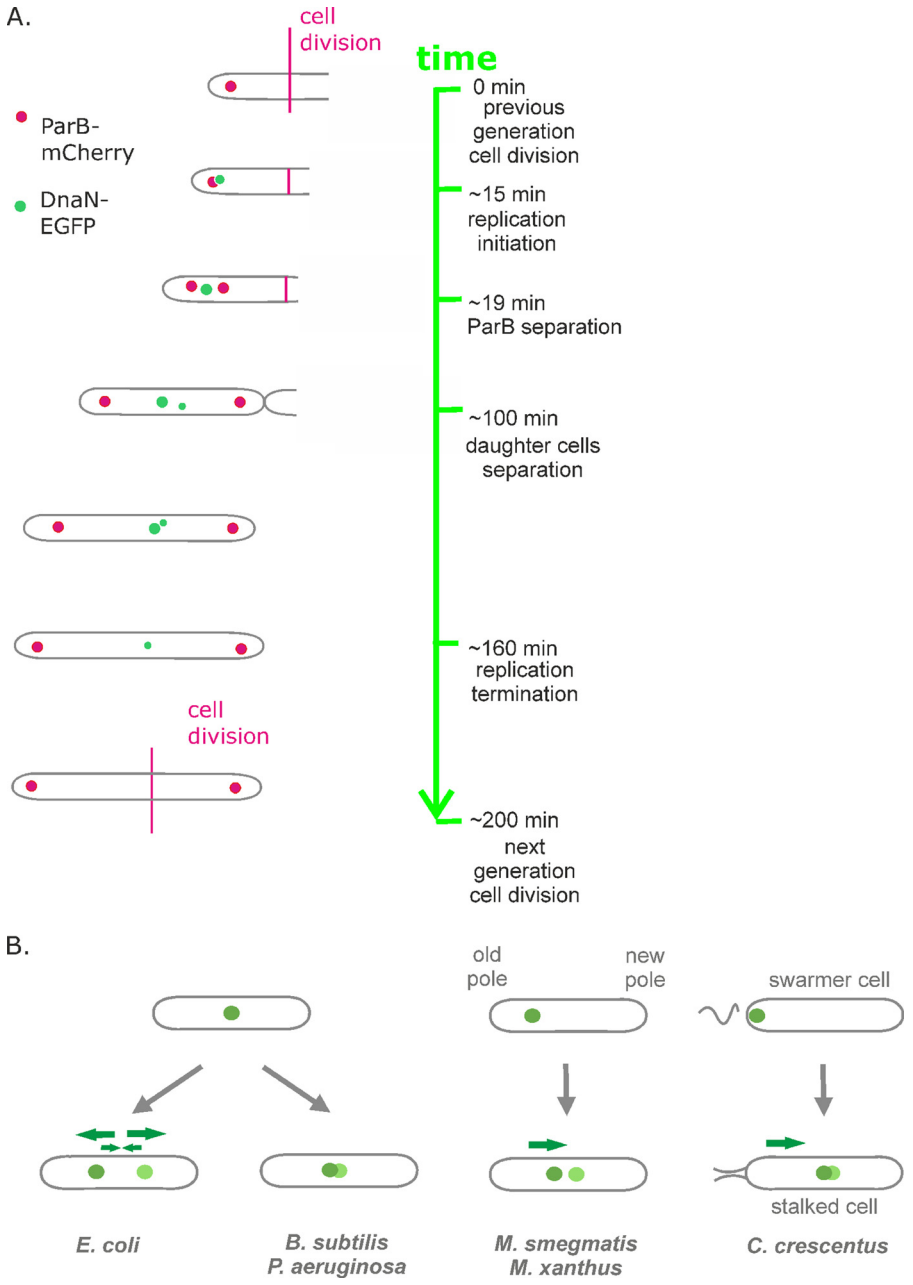

FIG 7 Dynamics of bacterial chromosome replication. (A) Cartoon illustrating key stages of chromosome replication during the *M. smegmatis* cell cycle. (B) Comparison of replisome positioning in different bacteria. Green arrows indicate directions of replisome movement.

together by intersister linkages before partitioning into daughter cells (31); this cohesion of newly replicated origins, which is similar to the chromosome adhesion observed in eukaryotes, lasts up to 20 to 30 min (32–34). Recent studies suggest that cohesion in *E. coli* is controlled by the DNA decatenation enzyme Topo IV and the protein SeqA (31), the latter of which is also involved in the regulation of replication initiation (35, 36). Notably, *E. coli*, in contrast to *M. smegmatis* and other bacteria, does not possess a ParABS system.

In *C. crescentus* and *B. subtilis*, only one replisome is visible throughout the cell cycle, in contrast, the replisomes in *M. smegmatis* split during cell elongation, though they are separated by only a short distance (10 to 20% of the cell length) relative to that in *E. coli* (about 50% of the cell length) (9). Their positions are also highly dynamic; replisomes "oscillate" around each other, frequently splitting and merging. During the course of a replication cycle, the position of replisomes shifts slightly toward the center of the cell (Fig. 3 to 5), whereas *oriC* regions are located at positions corresponding to 20 to 25% and 75 to 80% of the total cell length (17; data not shown). Replication is terminated near the cell center—the future division site. In addition, we observed a small fraction (10%) of cells with more than two DnaN-EGFP foci (Fig. 1A). This phenomenon might arise via the association of the DnaN clamp with DNA after the Okazaki fragment is synthesized on the

lagging strand. However, it was recently shown that the DnaN clamp also participates in other processes, such as DNA repair and recombination (6 37, 38).

Recent studies have shown that replisome positioning differs among bacteria (see Fig. 7B). Chromosome replication begins at specific cellular locations, which are different in various bacterial species, occurring at midcell in some bacteria (e.g., *B. subtilis*, *E. coli*, *Pseudomonas aeruginosa*) (39) and at the cell pole in others (e.g., *C. crescentus*, chromosome I of *V. cholerae*, *Helicobacter pylori*) (4, 12, 40). The positioning of sister replisomes also varies during the replication cycle (Fig. 7B). They stay together at the site of initiation during the course of replication in some species (e.g., *B. subtilis*, *P. aeruginosa*) and travel together to the midcell in others (e.g., *C. crescentus*, *H. pylori*). In *E. coli*, the sister replisomes move toward opposite poles. Interestingly, replisome dynamics in *M. smegmatis* combine different features from other bacteria: the two replisomes are physically separated, as in *E. coli*, but they move in the same direction from a subpolar region toward the cell center, as they do in *C. crescentus*. Similar hybrid replisome dynamics have recently been described in *M. xanthus* (27).

As expected, our data confirm that ParB, which participates in chromosome segregation and positioning of the *oriC* region, might also contribute to the localization of newly assembled replisomes (Fig. 6C). Indeed, ParB complexes in *M. smegmatis* are visible in newborn cells before replication initiation. In *C. crescentus*, the ParB-*parS* complex is tethered to PopZ at the old pole prior to the initiation of chromosome replication (41). Thus, in this bacterium, replisomes are assembled at the old cell pole. This process is similar to that observed in *V. cholerae*, where initiation of chromosome I replication takes place at one of the cell poles. In this bacterium, the recently identified protein HubP (hub of the pole) presumably controls the polar localization of the *oriCI* region by anchoring a ParA-like ATPase to the cell poles (42).

It remains unclear what is responsible for subcellular positioning of the replication machinery during replication in bacteria. It had previously been postulated that replisomes, similar to the *oriC* region, might be anchored by the cell membrane, but there is no evidence to support that hypothesis. Since replication must be coordinated with other key steps of the cell cycle, it is tempting to speculate that proteins (or protein complexes) involved in chromosome segregation and/or cell division participate directly or indirectly in replisome positioning. Interestingly, in *M. smegmatis*, elimination of ParB protein not only leads to aberrations in the positioning of newly assembled replisomes but also increases the distance between sister replisomes (Fig. 6A and B). Furthermore, ParB overproduction results in an increased number of cells without any replisomes (21%) or with more than two replisomes (23%) (Fig. 6F). Mycobacterial ParB has been suggested to form a compact complex in the *oriC*-proximal region (43). An excess of ParB presumably leads to the formation of massive ParB-*parS* complexes (see Movie S5) that may act through steric hindrance to prevent replisome assembly in newborn cells or disturb replisome movement during DNA synthesis. We speculate that disturbances in replisome movement caused by ParB overproduction generate a local accumulation of Okazaki fragments, which might be visible as additional foci (frequently weak and small). Moreover, asynchronous initiation of chromosome replication is frequently observed in daughter cells (see Movie S5), suggesting that changes in ParB levels influence the overall chromosome organization, which presumably affects the positioning of replisomes. A number of reports based on studies of other bacterial species confirm that ParB complexes serve an important function in overall nucleoid organization (44–47); in *B. subtilis*, it has been suggested that the recruitment of structural maintenance of chromosomes (SMC) by ParB may account for this phenomenon. A disturbed nucleoid architecture might also be a factor that affects replisome positioning and the distance between replisomes in *M. smegmatis* cells expressing altered ParB levels.

In summary, *M. smegmatis* cells, similar to eukaryote cells but in contrast to fast-growing bacterial cells, do not exhibit overlapping replication cycles. In *M. smegmatis*, replisomes track independently of each other, as is the case in *E. coli* and *M. xanthus* but not in *C. crescentus*. However, the overall movement of the two replisomes is similar to that in *C. crescentus* and *M. xanthus*. In each case, replisomes are highly dynamic; they change positions slightly, moving in the same direction from the old-pole-proximal cell half to the midcell. Moreover, our data suggest that ParB-assisted *oriC* localization not only determines the positioning of replisomes at the initiation of replication but also affects their behavior during the elongation phase, suggesting that ParB influences the overall chromosome organization in the cell and the synchronization of replication initiation.

MATERIALS AND METHODS

DNA manipulations, bacterial strains, and culture conditions. DNA manipulations were carried out by using standard protocols (48). Enzymes and chemicals were supplied by Thermo Scientific, Roth, and Sigma-Aldrich; oligonucleotides were synthesized by GenoMed or Sigma-Aldrich. The sequences of all PCR-derived clones were verified by DNA sequencing. Bacterial strains, plasmids, and oligonucleotides, as well as their relevant characteristics, are provided in Table S1 in the supplemental material. *E. coli* strains were grown in Luria-Bertani medium at 37°C. *M. smegmatis* mc^{2}155 and its derivatives were grown at 37°C in Middlebrook 7H9 broth (Difco) supplemented with 10% OADC (oleic acid-albumin-dextrose-catalase) and 0.05% Tween 80 or on 7H10 agar plates supplemented with 10% OADC and 0.5% glycerol. Growth of the strains analyzed was assayed (in at least triplicate) in a Bioscreen instrument for 24 h. Details of plasmid and strain construction are provided in Text S1 and Table S1 in the supplemental material.

Pulse-chase experiments. The protocol for pulse-chase labeling was similar to that previously described by Aldridge et al. (20). Briefly, bacteria were cultured overnight at 37°C in liquid medium to an optical density at 600 nm (OD_{600}) of 0.5. A 2-ml aliquot of the culture was centrifuged (8,000 rpm, 5 min, room temperature), washed, and resuspended in 200 μl of phosphate-buffered saline (PBS). For cell wall labeling, 1 μl of Alexa Fluor 488 succinimidyl ester isomer mix (Life Sciences) was added to the cell suspension to a final concentration of 0.05 mg/ml, mixed thoroughly, and immediately centrifuged at 8,000 rpm for 5 min. The cell pellet was resuspended in fresh 7H9-OADC medium, prewarmed to 37°C, and incubated for 2.5 h at 37°C. Subsequent steps were similar to those used to prepare samples for live microscopic snapshots (see below).

Microscopy analysis. For live-cell snapshot imaging, *M. smegmatis* was grown to mid-log phase (OD_{600} of 0.5) or late stationary phase (OD_{600} of 2.0) in liquid medium, centrifuged (8,000 rpm, 5 min), resuspended in PBS, and smeared onto microscope slides. After drying, samples were coverslip mounted with 5 μl of a PBS-glycerol (1:1) solution and visualized with a Zeiss Axio Imager Z1 fluorescence microscope equipped with a 100× objective. Snapshots were taken with AxioVision (Carl Zeiss) and analyzed with the MicrobeTracker suite (49).

TLMM. Microfluidic bacterial cell culture was performed in B04A plates with an ONIX flow control system (Merck-Millipore). Early-logarithmic-phase cells (OD_{600} of 0.2) were loaded into the flow chamber and cultured with continuous flow (pressure, 5 lb/in^2) in 7H9-OADC

medium at 37°C as described by the manufacturer. Images were recorded every 2, 10, or 20 min with either an inverted Zeiss Axio Observer fluorescence microscope (Carl Zeiss) equipped with a 100× oil immersion objective or a Delta Vision Elite inverted microscope with a 100× oil immersion objective. Images were analyzed with Zen software and/or the ImageJ Fiji suite (http://fiji.sc/Fiji). Data were analyzed with the R suite (R Foundation for Statistical Computing, Vienna, Austria; http://www.R-project.org), including the Peaks package (R package version 0.2 [M. Morhac, 2012]) and ggplot2 (50).

SUPPLEMENTAL MATERIAL

Supplemental material for this article may be found at http://mbio.asm.org/lookup/suppl/doi:10.1128/mBio.02125-14/-/DCSupplemental.

Text S1, DOC file, 0.04 MB.
Figure S1, JPG file, 0.6 MB.
Figure S2, JPG file, 0.4 MB.
Figure S3, JPG file, 0.3 MB.
Table S1, DOCX file, 0.1 MB.
Movie S1, MOV file, 3.2 MB.
Movie S2, MOV file, 18.5 MB.
Movie S3, MOV file, 18.7 MB.
Movie S4, MOV file, 0.9 MB.
Movie S5, MOV file, 6.4 MB.

ACKNOWLEDGMENTS

We are grateful to Agnieszka Strzałka for assistance with data analysis with the R statistical programming language. We thank Brian Robertson for providing the PBP1a expression plasmid.

This work was supported by the National Science Center, Poland (MAESTRO grant 2012/04/A/NZ1/00057). Damian Trojanowski is a fellow of the Akademia Rozwoju—kluczem wzmocnienia kadr polskiej gospodarki project, which was founded by the European Union from European Social Founds. The cost of publication was financed by the Wroclaw Centre of Biotechnology, programme of the Leading National Research Centre (KNOW) for years 2014–2018.

REFERENCES

1. **Gerdes K, Howard M, Szardenings F.** 2010. Pushing and pulling in prokaryotic DNA segregation. Cell **141:**927–942. http://dx.doi.org/10.1016/j.cell.2010.05.033.
2. **Thanbichler M.** 2010. Synchronization of chromosome dynamics and cell division in bacteria. Cold Spring Harb Perspect Biol **2:**a000331. http://dx.doi.org/10.1101/cshperspect.a000331.
3. **Imai Y, Ogasawara N, Ishigo-Oka D, Kadoya R, Daito T, Moriya S.** 2000. Subcellular localization of DNA-initiation proteins of *Bacillus subtilis*: evidence that chromosome replication begins at either edge of the nucleoids. Mol Microbiol **36:**1037–1048. http://dx.doi.org/10.1046/j.1365-2958.2000.01928.x.
4. **Jensen RB, Wang SC, Shapiro L.** 2001. A moving DNA replication factory in Caulobacter crescentus. EMBO J **20:**4952–4963. http://dx.doi.org/10.1093/emboj/20.17.4952.
5. **Lemon KP, Grossman AD.** 1998. Localization of bacterial DNA polymerase: evidence for a factory model of replication. Science **282:**1516–1519. http://dx.doi.org/10.1126/science.282.5393.1516.
6. **Reyes-Lamothe R, Sherratt DJ, Leake MC.** 2010. Stoichiometry and architecture of active DNA replication machinery in *Escherichia coli*. Science **328:**498–501. http://dx.doi.org/10.1126/science.1185757.
7. **Wang X, Lesterlin C, Reyes-Lamothe R, Ball G, Sherratt DJ.** 2011. Replication and segregation of an *Escherichia coli* chromosome with two replication origins. Proc Natl Acad Sci U S A **108:**E243–E250. http://dx.doi.org/10.1073/pnas.1100874108.
8. **Bates D, Kleckner N.** 2005. Chromosome and replisome dynamics in *E. coli*: loss of sister cohesion triggers global chromosome movement and mediates chromosome segregation. Cell **121:**899–911. http://dx.doi.org/10.1016/j.cell.2005.04.013.
9. **Reyes-Lamothe R, Possoz C, Danilova O, Sherratt DJ.** 2008. Independent positioning and action of *Escherichia coli* replisomes in live cells. Cell **133:**90–102. http://dx.doi.org/10.1016/j.cell.2008.01.044.
10. **Lemon KP, Grossman AD.** 2000. Movement of replicating DNA through a stationary replisome. Mol Cell **6:**1321–1330. http://dx.doi.org/10.1016/S1097-2765(00)00130-1.
11. **Migocki MD, Lewis PJ, Wake RG, Harry EJ.** 2004. The midcell replication factory in *Bacillus subtilis* is highly mobile: implications for coordinating chromosome replication with other cell cycle events. Mol Microbiol **54:**452–463. http://dx.doi.org/10.1111/j.1365-2958.2004.04267.x.
12. **Stokke C, Waldminghaus T, Skarstad K.** 2011. Replication patterns and organization of replication forks in Vibrio cholerae. Microbiology **157:**695–708. http://dx.doi.org/10.1099/mic.0.045112-0.
13. **Fossum S, Crooke E, Skarstad K.** 2007. Organization of sister origins and replisomes during multifork DNA replication in *Escherichia coli*. EMBO J **26:**4514–4522. http://dx.doi.org/10.1038/sj.emboj.7601871.
14. **Hayes F, Barillà D.** 2006. The bacterial segrosome: a dynamic nucleoprotein machine for DNA trafficking and segregation. Nat Rev Microbiol **4:**133–143. http://dx.doi.org/10.1038/nrmicro1342.
15. **Toro E, Shapiro L.** 2010. Bacterial chromosome organization and segregation. Cold Spring Harb Perspect Biol **2:**a000349. http://dx.doi.org/10.1101/cshperspect.a000349.
16. **Santi I, Dhar N, Bousbaine D, Wakamoto Y, McKinney JD.** 2013. Single-cell dynamics of the chromosome replication and cell division cycles in mycobacteria. Nat J Commun **4:**2470. http://dx.doi.org/10.1038/ncomms3470.
17. **Ginda K, Bezulska M, Ziółkiewicz M, Dziadek J, Zakrzewska-Czerwińska J, Jakimowicz D.** 2013. ParA of Mycobacterium smegmatis co-ordinates chromosome segregation with the cell cycle and interacts with the polar growth determinant DivIVA. Mol Microbiol **87:**998–1012. http://dx.doi.org/10.1111/mmi.12146.
18. **Thanky NR, Young DB, Robertson BD.** 2007. Unusual features of the cell cycle in mycobacteria: polar-restricted growth and the snapping-model of cell division. Tuberculosis (Edinb) **87:**231–236. http://dx.doi.org/10.1016/j.tube.2006.10.004.
19. **Daniel RA, Errington J.** 2003. Control of cell morphogenesis in bacteria: two distinct ways to make a rod-shaped cell. Cell **113:**767–776. http://dx.doi.org/10.1016/S0092-8674(03)00421-5.
20. **Aldridge BB, Fernandez-Suarez M, Heller D, Ambravaneswaran V, Irimia D, Toner M, Fortune SM.** 2012. Asymmetry and aging of mycobacterial cells lead to variable growth and antibiotic susceptibility. Science **335:**100–104. http://dx.doi.org/10.1126/science.1216166.
21. **Joyce G, Williams KJ, Robb M, Noens E, Tizzano B, Shahrezaei V, Robertson BD.** 2012. Cell division site placement and asymmetric growth in mycobacteria. PLoS One **7:**e44582. http://dx.doi.org/10.1371/journal.pone.0044582.
22. **Zawilak A, Kois A, Konopa G, Smulczyk-Krawczyszyn A, Zakrzewska-Czerwińska J.** 2004. Mycobacterium tuberculosis DnaA initiator protein: purification and DNA-binding requirements. Biochem J **382:**247–252. http://dx.doi.org/10.1042/BJ20040338.
23. **Kumar S, Farhana A, Hasnain SE.** 2009. In-vitro helix opening of M. tuberculosis oriC by DnaA occurs at precise location and is inhibited by IciA like protein. PLoS One **4:**e4139. http://dx.doi.org/10.1371/journal.pone.0004139.
24. **Dziedzic R, Kiran M, Plocinski P, Ziolkiewicz M, Brzostek A, Moomey M, Vadrevu IS, Dziadek J, Madiraju M, Rajagopalan M.** 2010. Mycobacterium tuberculosis ClpX interacts with FtsZ and interferes with FtsZ assembly. PLoS One **5:**e11058. http://dx.doi.org/10.1371/journal.pone.0011058.
25. **Jakimowicz D, Brzostek A, Rumijowska-Galewicz A, Zydek P, Dołżbłasz A, Smulczyk-Krawczyszyn A, Zimniak T, Wojtasz L, Zawilak-Pawlik A, Kois A, Dziadek J, Zakrzewska-Czerwińska J.** 2007. Characterization of the mycobacterial chromosome segregation protein ParB and identification of its target in Mycobacterium smegmatis. Microbiol Read Engl **153:**4050–4060. http://dx.doi.org/10.1099/mic.0.2007/011619-0.
26. **Jackson D, Wang X, Rudner DZ.** 2012. Spatio-temporal organization of replication in bacteria and eukaryotes (nucleoids and nuclei). Cold Spring Harb Perspect Biol **4:**a010389. http://dx.doi.org/10.1101/cshperspect.a010389.
27. **Harms A, Treuner-Lange A, Schumacher D, Søgaard-Andersen L.** 2013. Tracking of chromosome and replisome dynamics in Myxococcus xanthus reveals a novel chromosome arrangement. PLoS Genet **9:**e1003802. http://dx.doi.org/10.1371/journal.pgen.1003802.
28. **Dingwall A, Shapiro L.** 1989. Rate, origin, and bidirectionality of Caulobacter chromosome replication as determined by pulsed-field gel electro-

phoresis. Proc Natl Acad Sci U S A **86:**119–123. http://dx.doi.org/10.1073/pnas.86.1.119.
29. **Hiriyanna KT, Ramakrishnan T.** 1986. Deoxyribonucleic acid replication time in Mycobacterium tuberculosis H37 Rv. Arch Microbiol **144:** 105–109. http://dx.doi.org/10.1007/BF00414718.
30. **Nair N, Dziedzic R, Greendyke R, Muniruzzaman S, Rajagopalan M, Madiraju MV.** 2009. Synchronous replication initiation in novel Mycobacterium tuberculosis dnaA cold-sensitive mutants. Mol Microbiol **71:** 291–304. http://dx.doi.org/10.1111/j.1365-2958.2008.06523.x.
31. **Joshi MC, Magnan D, Montminy TP, Lies M, Stepankiw N, Bates D.** 2013. Regulation of sister chromosome cohesion by the replication fork tracking protein SeqA. PLoS Genet **9:**e1003673. http://dx.doi.org/10.1371/journal.pgen.1003673.
32. **Espeli O, Mercier R, Boccard F.** 2008. DNA dynamics vary according to macrodomain topography in the *E. coli* chromosome. Mol Microbiol **68:** 1418–1427. http://dx.doi.org/10.1111/j.1365-2958.2008.06239.x.
33. **Joshi MC, Bourniquel A, Fisher J, Ho BT, Magnan D, Kleckner N, Bates D.** 2011. *Escherichia coli* sister chromosome separation includes an abrupt global transition with concomitant release of late-splitting intersister snaps. Proc Natl Acad Sci U S A **108:**2765–2770. http://dx.doi.org/10.1073/pnas.1019593108.
34. **Nielsen HJ, Li Y, Youngren B, Hansen FG, Austin S.** 2006. Progressive segregation of the *Escherichia coli* chromosome. Mol Microbiol **61:** 383–393. http://dx.doi.org/10.1111/j.1365-2958.2006.05245.x.
35. **Lu M, Campbell JL, Boye E, Kleckner N.** 1994. SeqA: a negative modulator of replication initiation in *E. coli*. Cell **77:**413–426. http://dx.doi.org/10.1016/0092-8674(94)90156-2.
36. **Slater S, Wold S, Lu M, Boye E, Skarstad K, Kleckner N.** 1995. *E. coli* SeqA protein binds oriC in two different methyl-modulated reactions appropriate to its roles in DNA replication initiation and origin sequestration. Cell **82:**927–936. http://dx.doi.org/10.1016/0092-8674(95)90272-4.
37. **López de Saro FJ, O'Donnell M.** 2001. Interaction of the beta sliding clamp with MutS, ligase, and DNA polymerase I. Proc Natl Acad Sci U S A **98:**8376–8380. http://dx.doi.org/10.1073/pnas.121009498.
38. **Simmons LA, Davies BW, Grossman AD, Walker GC.** 2008. Beta clamp directs localization of mismatch repair in *Bacillus subtilis*. Mol Cell **29:** 291–301. http://dx.doi.org/10.1016/j.molcel.2007.10.036.
39. **Vallet-Gely I, Boccard F.** 2013. Chromosomal organization and segregation in *Pseudomonas aeruginosa*. PLoS Genet **9:**e1003492. http://dx.doi.org/10.1371/journal.pgen.1003492.
40. **Sharma A, Kamran M, Verma V, Dasgupta S, Dhar SK.** 2014. Intracellular locations of replication proteins and the origin of replication during chromosome duplication in the slowly growing human pathogen *Helicobacter pylori*. J Bacteriol **196:**999–1011. http://dx.doi.org/10.1128/JB.01198-13.
41. **Ptacin JL, Gahlmann A, Bowman GR, Perez AM, von Diezmann AR, Eckart MR, Moerner WE, Shapiro L.** 2014. Bacterial scaffold directs pole-specific centromere segregation. Proc Natl Acad Sci U S A **111:** E2046–E2055. http://dx.doi.org/10.1073/pnas.1405188111.
42. **Yamaichi Y, Bruckner R, Ringgaard S, Möll A, Cameron DE, Briegel A, Jensen GJ, Davis BM, Waldor MK.** 2012. A multidomain hub anchors the chromosome segregation and chemotactic machinery to the bacterial pole. Genes Dev **26:**2348–2360. http://dx.doi.org/10.1101/gad.199869.112.
43. **Chaudhuri BN, Dean R.** 2011. The evidence of large-scale DNA-induced compaction in the mycobacterial chromosomal ParB. J Mol Biol **413:** 901–907. http://dx.doi.org/10.1016/j.jmb.2011.08.002.
44. **Broedersz CP, Wang X, Meir Y, Loparo JJ, Rudner DZ, Wingreen NS.** 2014. Condensation and localization of the partitioning protein ParB on the bacterial chromosome. Proc Natl Acad Sci U S A **111:**8809–8814. http://dx.doi.org/10.1073/pnas.1402529111.
45. **Graham TG, Wang X, Song D, Etson CM, van Oijen AM, Rudner DZ, Loparo JJ.** 2014. ParB spreading requires DNA bridging. Genes Dev **28:** 1228–1238. http://dx.doi.org/10.1101/gad.242206.114.
46. **Lee PS, Grossman AD.** 2006. The chromosome partitioning proteins Soj (ParA) and Spo0J (ParB) contribute to accurate chromosome partitioning, separation of replicated sister origins, and regulation of replication initiation in *Bacillus subtilis*. Mol Microbiol **60:**853–869. http://dx.doi.org/10.1111/j.1365-2958.2006.05140.x.
47. **Umbarger MA, Toro E, Wright MA, Porreca GJ, Baù D, Hong S-H, Fero MJ, Zhu LJ, Marti-Renom MA, McAdams HH, Shapiro L, Dekker J, Church GM.** 2011. The three-dimensional architecture of a bacterial genome and its alteration by genetic perturbation. Mol Cell **44:**252–264. http://dx.doi.org/10.1016/j.molcel.2011.09.010.
48. **Sambrook J, Russell DW.** 2001. Molecular cloning: a laboratory manual, 3rd ed. Cold Spring Harbor Laboratory Press, Cold Spring Harbor, NY.
49. **Sliusarenko O, Heinritz J, Emonet T, Jacobs-Wagner C.** 2011. High-throughput, subpixel precision analysis of bacterial morphogenesis and intracellular spatio-temporal dynamics. Mol Microbiol **80:**612–627. http://dx.doi.org/10.1111/j.1365-2958.2011.07579.x.
50. **Wickham H.** 2009. ggplot2: elegant graphics for data analysis (use R!). Springer, New York, NY.